

EXTENDED-STATE-OBSERVER-BASED CONSTRAINED CONTROL FOR A CLASS OF NONLINEAR SYSTEMS: A BACKSTEPPING APPROACH

NAN JI^{1,2}, DEZHI XU^{1,2} AND FEI LIU^{1,2}

¹Key Laboratory of Advanced Process Control for Light Industry (Ministry of Education)

²Institute of Automation

Jiangnan University

No. 1800, Lihu Avenue, Wuxi 214122, P. R. China

lutxdz@126.com

Received November 2015; accepted February 2016

ABSTRACT. *This brief studies the output tracking control problem for a class of unknown nonlinear systems subject to actuator magnitude and rate saturation. We first design multiple extended state observers (ESOs) which are used to identify nonlinear time-varying dynamic model. Then, based on ESOs, we apply the command-filtered backstepping technique to constructing a constrained nonlinear control law to solve the problem. Our constrained control law contains command filter for eliminating the impact of derivative and control saturation, and we will show that tracking errors are asymptotically convergent. Finally, a two-link robot manipulator is used to demonstrate that the proposed constrained control algorithm has a very reliable tracking ability and a satisfactory robustness and process dynamics variations.*

Keywords: Actuator saturation, Nonlinear control, Extended state observer (ESO), Command-filtered backstepping, Uncertainties

1. Introduction. Input saturation problem is widely presented in many practical control systems [1-4]. If input saturation is ignored in the control design, the close-loop system could become unstable. Hence, many researchers have focused on study of various control problems subject to actuator saturation [1-9]. We all know, a large number of actual control systems are nonlinear and multiple-input-multiple-output (MIMO). And actuator rate saturation can also cause instability for closed-loop control systems. However, most of the research achievements of input saturation are mainly concentrated on linear systems and actuator magnitude constraint problem; the saturation problems of nonlinear systems and rate constraint problem are still difficult points.

In control theory, backstepping is a technique developed in 1990s for designing stabilizing controls for a special class of nonlinear dynamical systems [10]. These systems are built from subsystems that radiate out from an irreducible subsystem that can be stabilized using some other method [11]. There are differential expansion and constraint problems in traditional backstepping control. Therefore, in recent years, many research results have been reported (see, for instance, [12-14] and the references therein).

Since natural dynamic process is highly complex nonlinear, the precise dynamic mathematical model is difficult to be obtained. In recent years, many researchers start to draw their attention to model-free control [8,9,15]. Although adaptive technique-based fuzzy logic and neural network have been intensively researched for nonlinear systems in the last two decades [16,17], there is still no assurance of high convergence speed, the overheating phenomenon and so on; meanwhile, there are no general methods to choose the number of the fuzzy rule base and hidden units of common neural network.

In this brief paper, a novel constrained nonlinear control scheme with extended state observer (ESO) using command-filtered backstepping technique, is proposed for tracking

control tasks. In our method, multiple ESOs are used to observe states and unknown nonlinear time-varying function vector. In doing so, a new variable vector is introduced for designing constrained controller. The proposed approach has several advantages, which make this method suitable for control applications. First, it just depends on the real-time measurement output of the controlled plant. Second, it does not require precise dynamic mathematical model and other testing signals. Third, it is simple and easily implementable with small computational burden and has strong robustness.

The remainder of this brief is organized as follows. In Section 2, problem formulation is given; main results are presented in Section 3. Section 4 gives a two-link robot manipulator simulation example. The conclusions are drawn in the last section.

2. Problem Formulation. Consider the following MIMO nonlinear system as

$$\begin{aligned} \ddot{y}_1 &= f_1(y_1, \dot{y}_1, \dots, y_m, \dot{y}_m, t) + B_1 U \\ \ddot{y}_2 &= f_2(y_1, \dot{y}_1, \dots, y_m, \dot{y}_m, t) + B_2 U \\ &\dots \\ \ddot{y}_m &= f_m(y_1, \dot{y}_1, \dots, y_m, \dot{y}_m, t) + B_m U \end{aligned} \quad (1)$$

Define $Y = [y_1, y_2, \dots, y_m]^T$, $X = [X_1, X_2]^T = [Y^T, \dot{Y}^T]^T$, $U = [u_1, u_2, \dots, u_m]^T$, and

$$F(X, t) = \begin{pmatrix} f_1(y_1, \dot{y}_1, \dots, y_m, \dot{y}_m, t) \\ f_2(y_1, \dot{y}_1, \dots, y_m, \dot{y}_m, t) \\ \vdots \\ f_m(y_1, \dot{y}_1, \dots, y_m, \dot{y}_m, t) \end{pmatrix}, \quad B = \begin{pmatrix} B_1 \\ B_2 \\ \vdots \\ B_m \end{pmatrix} = \begin{pmatrix} b_{11} & b_{12} & \dots & b_{1m} \\ b_{21} & b_{22} & \dots & b_{2m} \\ \vdots & \vdots & \ddots & \vdots \\ b_{m1} & b_{m2} & \dots & b_{mm} \end{pmatrix}$$

Hence, system (1) also can be described as follows

$$\dot{X}_1 = X_2, \quad \dot{X}_2 = F(X, t) + BU, \quad Y = X_1 \quad (2)$$

In practice, because the input of the controlled plant (1) cannot change too fast within a small time interval due to the ‘‘inertia’’ of the actuator. The control inputs are subject to magnitude and rate constraint as follows

$$a_{\min} \leq U \leq a_{\max}, \quad \delta_{\min} \leq \dot{U} \leq \delta_{\max} \quad (3)$$

where a_{\min} and a_{\max} are the minimum and maximum values of magnitude constraints of the control inputs. δ_{\min} and δ_{\max} are the minimum and maximum values of rate constraints of the control inputs.

3. Main Results.

3.1. ESO design. For the following i th ($i = 1, 2, \dots, m$) subsystem of Equation (1),

$$\ddot{y}_i = f_i(y_1, \dot{y}_1, \dots, y_m, \dot{y}_m) + B_i U \quad (4)$$

Define $x_{i1} = y_i$, $x_{i2} = \dot{y}_i$, and then, it can be written as state space by

$$\dot{x}_{i1} = x_{i2}, \quad \dot{x}_{i2} = f_i(X, t) + B_i U, \quad y_i = x_{i1} \quad (5)$$

Because $f_i(\cdot)$ and state x_2 are unknown, the third-order ESO is designed, which is used to estimate the state x_2 and unknown function $f_i(\cdot)$. Define the unknown function $f_i(\cdot)$ as an extended state x_{i3} . Let $x_{i3} = f_i(X, t)$, $\dot{x}_{i3} = \omega_i$, and we assume that $|\omega_i(t)| < r$. Then system (5) is equivalent to

$$\dot{x}_{i1} = x_{i2}, \quad \dot{x}_{i2} = f_i(X, t) + B_i U, \quad \dot{x}_{i3} = \omega_i, \quad y_i = x_{i1} \quad (6)$$

In order to estimate the state x_{i2} and unknown function $f_i(X, t)$, we design the following third-order ESO [10,11]:

$$\begin{aligned} \dot{\hat{x}}_{i1} &= \hat{x}_{i2} - l_{i1}e_{i1} \\ \dot{\hat{x}}_{i2} &= \hat{x}_{i3} + B_iU - l_{i2}\text{fal}(e_{i1}, \alpha_{i1}, \sigma_{i1}) \\ \dot{\hat{x}}_{i3} &= -l_{i3}\text{fal}(e_{i1}, \alpha_{i2}, \sigma_{i2}) \\ \hat{y}_i &= \hat{x}_{i1} \end{aligned} \tag{7}$$

where $e_{i1} = y_i - \hat{y}_i = x_{i1} - \hat{x}_{i1}$ and $\hat{x}_{i1}, \hat{x}_{i2}, \hat{x}_{i3}$ are the observers of x_{i1}, x_{i2}, x_{i3} . $0 < \alpha_{i1} < 1$, $0 < \alpha_{i2} < 1$, $\sigma_{i1} > 0$, $\sigma_{i2} > 0$, $l_{ij} > 0$, $j = 1, 2, 3$ are parameters of observer (7). And the nonlinear function $\text{fal}(\cdot)$ is defined as

$$\text{fal}(e, \alpha, \sigma) = \begin{cases} |e|^\alpha \text{sgn}(e), & |e| > \sigma \\ \frac{e}{\sigma^{1-\alpha}}, & |e| \leq \sigma \end{cases} \tag{8}$$

where α includes α_{i1} and α_{i2} , e is e_{i1} , σ includes σ_{i1} and σ_{i2} . Let T be sampling period of control, in general, σ is selected as $\sigma = 5 \sim 10T$. Until now, there is no reliable theoretical analysis method available for third-order ESO. Fortunately, according to [18], if suitable parameters of observer (7) are selected, the following results can be obtained.

$$\begin{aligned} \lim_{t \rightarrow \infty} |\tilde{x}_{i2}| &< l_{i1} \left(\frac{r}{l_{i3}} \right)^{1/\alpha_{i2}} = \varepsilon_{x_{i2}} \\ \lim_{t \rightarrow \infty} |\tilde{x}_{i3}| &< l_{i2} \left(\frac{r}{l_{i3}} \right)^{1/\alpha_{i2}} = \varepsilon_{f_i(X,t)} \end{aligned} \tag{9}$$

where $\tilde{x}_{i2} = x_{i2} - \hat{x}_{i2}$, $\tilde{x}_{i3} = x_{i3} - \hat{x}_{i3}$. Hence, we know the suitable observer parameters can make the state estimation errors \tilde{x}_{i1} , \tilde{x}_{i2} and function estimation error $\tilde{f}_i(X, t) = \tilde{x}_{i3} = f_i(X, t) - \hat{f}_i(X, t)$ are uniformly ultimately bounded (UUB).

If m above suitable ESOs are designed for Equation (2), the estimation errors of $X_1, X_2, F(X, t)$ are ensured UUB. And the designed ESO of Equation (2) can be described as

$$\dot{\hat{X}}_1 = \hat{X}_2 + \Theta_1, \quad \dot{\hat{X}}_2 = \Theta_2 + BU \tag{10}$$

where

$$\Theta_1 = - \begin{pmatrix} l_{11}e_{11} \\ l_{21}e_{21} \\ \vdots \\ l_{m1}e_{m1} \end{pmatrix}, \quad \Theta_2 = \begin{pmatrix} \hat{x}_{13} - l_{12}\text{fal}(e_{11}, \alpha_{11}, \sigma_{11}) \\ \hat{x}_{23} - l_{22}\text{fal}(e_{21}, \alpha_{21}, \sigma_{21}) \\ \vdots \\ \hat{x}_{m3} - l_{m2}\text{fal}(e_{m1}, \alpha_{m1}, \sigma_{m1}) \end{pmatrix}$$

3.2. ESO based controller design and stability analysis. It can be seen that above Equation (10) is strict-feedback form, so we can design the controller via backstepping idea. Here, we introduce a new variable N , and make $\dot{U} = N$. Then Equation (10) can be extended as

$$\dot{\hat{X}}_1 = \hat{X}_2 + \Theta_1, \quad \dot{\hat{X}}_2 = \Theta_2 + BU, \quad \dot{U} = N \tag{11}$$

Define the tracking error variables E_1, E_2 and E_3 , which are introduced as follows

$$E_1 = \hat{X}_1 - X_1^c, \quad E_2 = \hat{X}_2 - \hat{X}_2^c, \quad E_3 = U - U^c \tag{12}$$

where X_1^c, \hat{X}_2^c and U^c are the command filtered version of trajectory tracking X_1 , virtual control signal \hat{X}_2^d and U^d , respectively. Considering differential expansion problem, the first-order command filter

$$\dot{\hat{X}}_2^c = \Lambda \left(\hat{X}_2^d - \hat{X}_2^c \right) \tag{13}$$

is employed to track the desired \hat{X}_2^d . The filter time constant matrix $\Lambda = \text{diag}\{\gamma_1, \gamma_2, \dots, \gamma_m\} > 0$ should be as large as possible to promise the fast tracking.

The control input U is subject to magnitude and rate constraints like (3). Here, we choose the constrained command filter to track the desired U^d [11], which is shown in Figure 1, the constrained command filter can eliminate the saturation of magnitude and rate of the control input via magnitude limiter and rate limiter, and the state-space model of constrained command filter can be described as

$$\begin{cases} \dot{q}_1 \\ \dot{q}_2 \end{cases} = \begin{bmatrix} q_2 \\ 2\xi\omega_n \left[S_R \left(\frac{\omega_n^2}{2\xi\omega_n} (S_M(u) - q_1) \right) - q_2 \right] \end{bmatrix} \quad (14)$$

where

$$\begin{bmatrix} q_1 \\ q_2 \end{bmatrix} = \begin{bmatrix} x^c \\ \dot{x}^c \end{bmatrix}, \quad u = x^d$$

$S_M(\cdot)$ and $S_R(\cdot)$ are saturation function of magnitude and rate respectively, and their upper and lower limits can be designed by constraints (3). ξ and ω_n are damping and bandwidth of filter respectively.

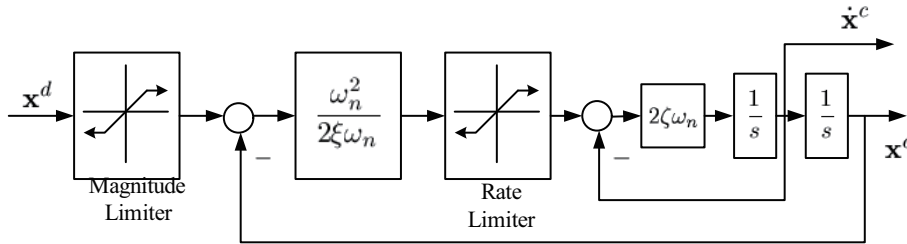


FIGURE 1. Structure of constrained command filters

Redefine tracking errors

$$\bar{E}_1 = E_1 - \epsilon_1, \quad \bar{E}_2 = E_2 - \epsilon_2 \quad (15)$$

where compensated filter errors ϵ_1 and ϵ_2 are designed as

$$\dot{\epsilon}_1 = -K_1\epsilon_1 + \hat{X}_2^c - \hat{X}_2^d + \epsilon_2 \quad (16)$$

$$\dot{\epsilon}_2 = -K_2\epsilon_2 + B(U^c - U^d) \quad (17)$$

where K_1 and K_2 are controller gain, which are designed later. From (12), and (15)-(17), we have

$$\dot{\bar{E}}_1 = \hat{X}_2 + \Theta_1 - \dot{\hat{X}}_1^c + K_1\epsilon_1 - \hat{X}_2^c + \hat{X}_2^d - \epsilon_2 \quad (18)$$

$$\dot{\bar{E}}_2 = BU + \Theta_2 - \dot{\hat{X}}_2^c + K_2\epsilon_2 - B(U^c - U^d) \quad (19)$$

$$\dot{\bar{E}}_3 = N - \dot{U}^c \quad (20)$$

The virtual control laws \hat{X}_2^d , U^d and global control law N are designed as

$$\hat{X}_2^d = \dot{\hat{X}}_1^c - \Theta_1 - K_1 E_1 \quad (21)$$

$$U^d = B^{-1} \left(-K_2 E_2 - \Theta_2 + \bar{E}_1 + \dot{\hat{X}}_2^c \right) \quad (22)$$

$$N = -K_3 E_3 + B^T \bar{E}_2 + \dot{U}^c \quad (23)$$

where K_1 , K_2 and K_3 are positive definite matrices.

Consider the Lyapunov function

$$V = \frac{1}{2} \bar{E}_1^T \bar{E}_1 + \frac{1}{2} \bar{E}_2^T \bar{E}_2 + \frac{1}{2} E_3^T E_3 \quad (24)$$

The time derivative of V with respect to time and substituting (21)-(23), it yields

$$\begin{aligned}\dot{V} &= \bar{E}_1^T \dot{\bar{E}}_1 + \bar{E}_2^T \dot{\bar{E}}_2 + E_3^T \dot{E}_3 \\ &= \bar{E}_1^T \left(\dot{\hat{X}}_2 + \Theta_1 - \dot{X}_1^c + K_1 \epsilon_1 - \dot{\hat{X}}_2^c + \dot{\hat{X}}_2^d - \epsilon_2 \right) \\ &\quad + \bar{E}_2^T \left(BU + \Theta_2 - \dot{\hat{X}}_2^c + K_2 \epsilon_2 - BU^c + BU^d \right) + E_3^T \left(N - \dot{U}^c \right) \\ &= -K_1 \|\bar{E}_1\|^2 - K_2 \|\bar{E}_2\|^2 + \bar{E}_2^T BE_3 + E_3^T \left(N - \dot{U}^c \right) \\ &= -K_1 \|\bar{E}_1\|^2 - K_2 \|\bar{E}_2\|^2 - K_3 \|E_3\|^2 \leq 0\end{aligned}$$

Through the above analysis, it can be seen that the tracking errors \bar{E}_1 , \bar{E}_2 , E_3 are asymptotic convergence.

From Equations (16) and (17), if it is sure that $\hat{X}_2^c - \hat{X}_2^d$ and $U^c - U^d$ are bounded, then ϵ_1 and ϵ_2 are bounded. Further E_1 and E_2 are bounded. Combined with the conclusion of Section 3.1, we can get the boundedness of all error signal.

To give a clear idea of the overall design procedure, we give a flow chart as Figure 2.

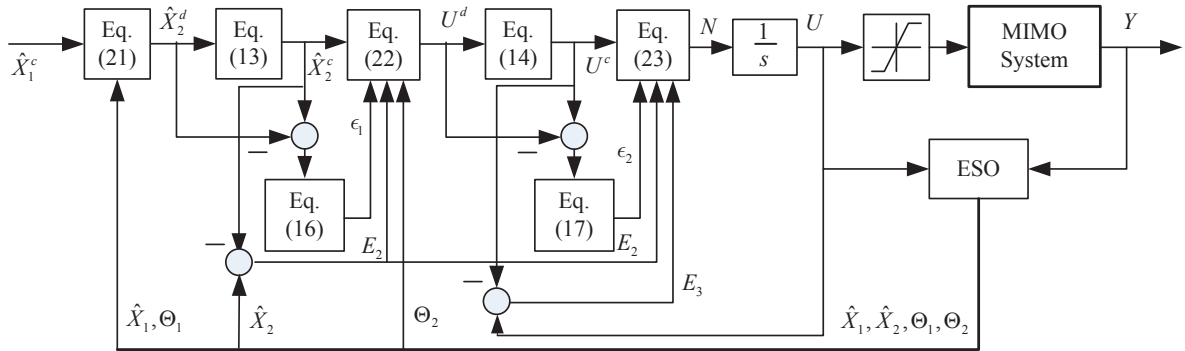


FIGURE 2. The flow chart of the design procedure

Remark 3.1. 1) The proposed ESO-based nonlinear control method does not need to know the differential signal \dot{Y} and unknown function vector $F(X, t)$.

2) So far, active disturbance rejection control (ADRC) has no strict stability proof [18]. In this paper, we give the stability analysis for the proposed control approach, and moreover the control constraint problem is considered.

3) Like ADRC, the proposed control algorithm does not need accurate control gain matrix B . Also, the developed control method can achieve the purpose of dynamic decoupling.

4. Simulation Results. In this section, simulation studies are carried out to show the effectiveness of the proposed ESO-based constrained nonlinear controller. Consider a two-link robot manipulator as shown in Figure 3, and its dynamic equation is given as follows [19]:

$$M(q)\ddot{q} + C(q, \dot{q})\dot{q} + G(q) = \tau \quad (25)$$

where

$$M(q) = \begin{bmatrix} (m_1 + m_2)l_1^2 & m_2l_1l_2(s_1s_2 + c_1c_2) \\ m_2l_1l_2(s_1s_2 + c_1c_2) & m_2l_2^2 \end{bmatrix},$$

$$C(q, \dot{q}) = m_2l_1l_2(c_1s_2 - s_1c_2) \begin{bmatrix} 0 & \dot{q}_2 \\ -\dot{q}_1 & 0 \end{bmatrix},$$

$$G(q) = \begin{bmatrix} -(m_1 + m_2)l_1gs_1 \\ -m_2l_2gs_2 \end{bmatrix},$$

and $q = [q_1, q_2]$, q_1, q_2 are generalized coordinates, $M(q)$ is the moment of inertia, $C(q, \dot{q})$ includes Coriolis, centripetal forces, and $G(q)$ is the gravitational force. Other quantities are: link mass m_1, m_2 , link length l_1, l_2 , angular position q_1, q_2 , applied torques $\tau = [\tau_1, \tau_2]^T$, the acceleration due to gravity $g = 9.8(\text{m/s}^2)$, and short-hand notation $s_1 = \sin(q_1)$, $s_2 = \sin(q_2)$, $c_1 = \cos(q_1)$ and $c_2 = \cos(q_2)$. Let $x_1 = q_1$, $x_2 = q_2$, $x_3 = \dot{q}_1$ and $x_4 = \dot{q}_2$. In simulation, two-link robot's parameters are given as $m_1 = m_2 = 0.5$, $l_1 = 1$ and $l_2 = 0.8$.

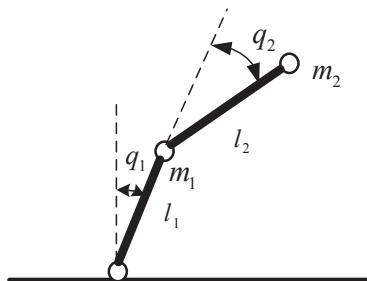


FIGURE 3. The configuration of two-link robot manipulator

Let $Y = X_1 = [x_1, x_2]^T$, $X_2 = [x_3, x_4]^T$, $U = [\tau_1, \tau_2]^T$. Then, system (25) can be expressed as follows:

$$\dot{X}_1 = X_2, \quad \dot{X}_2 = F(X, t) + BU, \quad Y = X_1$$

where $F(X, t) = -M^{-1}(q)(C(q, \dot{q})\dot{q} + G(q)) + (M^{-1}(q) - B)U$ and $F(X, t)$ is assumed unknown. In the simulation, B is chosen as

$$B = \begin{bmatrix} 2 & -4.5 \\ -4.5 & 13 \end{bmatrix}.$$

The initial conditions of the system are taken as $X(0) = [X_1^T(0), X_2^T(0)]^T = [0.5, 0.5, 0, 0]^T$. The desired trajectories are selected as $X_1^c = [\sin(2t), \sin(2t)]^T$. The constraints of control input U are

$$\begin{bmatrix} -20 \\ -8 \end{bmatrix} \leq U \leq \begin{bmatrix} 20 \\ 8 \end{bmatrix}, \quad \begin{bmatrix} -150 \\ -150 \end{bmatrix} \leq \dot{U} \leq \begin{bmatrix} 150 \\ 150 \end{bmatrix}.$$

The designed control parameters are chosen as

$$K_1 = K_2 = \begin{bmatrix} 10 & 0 \\ 0 & 15 \end{bmatrix}, \quad K_3 = \begin{bmatrix} 100 & 0 \\ 0 & 150 \end{bmatrix}.$$

The parameter of filter (13) is

$$\Lambda = \begin{bmatrix} 200 & 0 \\ 0 & 400 \end{bmatrix}.$$

The parameters of ESO are designed as $\alpha_{11} = \alpha_{12} = \alpha_{21} = \alpha_{22} = 0.9$, $\sigma_{11} = \sigma_{21} = 10$, $\sigma_{12} = \sigma_{22} = 100$, $l_{11} = l_{21} = 200$, $l_{12} = l_{22} = l_{13} = l_{23} = 10^5$. And constrained command filter parameters are shown in Table 1.

The simulation results for the first link are shown in Figure 4, and those for the second link are shown in Figure 5, where ‘‘ref.’’ is the preset reference trajectory. In Figure

TABLE 1. Constrained command filter parameters

Variables	ξ	ω_n	Mag. limit	Rate limit
u_1	1	50	± 20	± 150
u_2	1	50	± 8	± 150

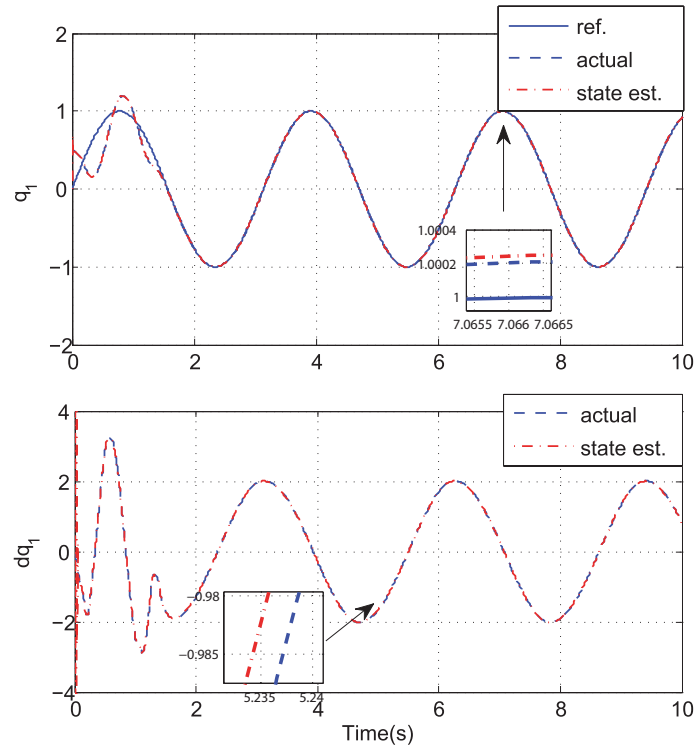


FIGURE 4. Tracking curves of link 1

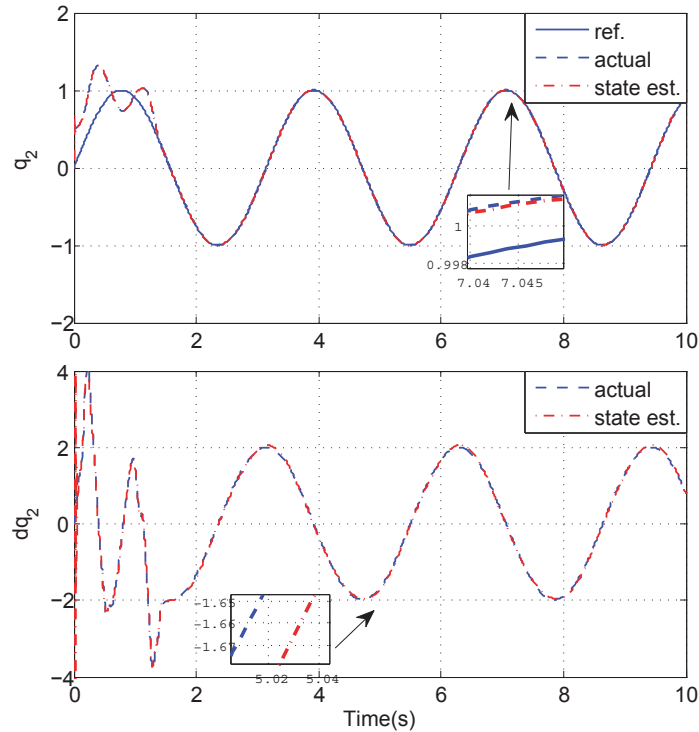


FIGURE 5. Tracking curves of link 2

4 and Figure 5, we can observe that the reference trajectories and actual responses of two links in robot manipulator almost overlap with each other, and the good tracking performance is obtained. The control input signals are shown in Figure 6, and we can see that the control signals are in constraints. These simulation results demonstrate the tracking capability of the proposed controller and its effectiveness for control tracking of constrained nonlinear systems.

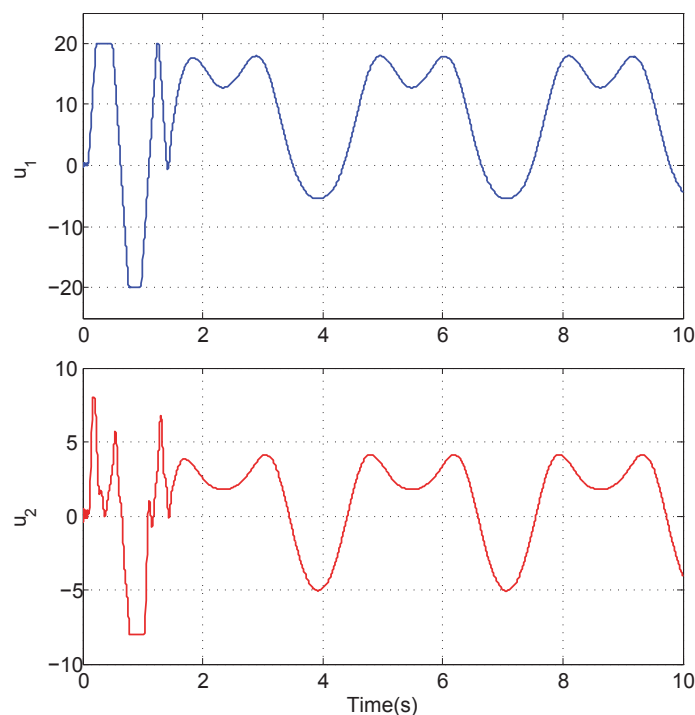


FIGURE 6. Control input signals

5. **Conclusion.** This brief has revisited the problem of output tracking control for a class unknown nonlinear systems subject to actuator saturation. Based on dynamic model of multiple ESOs and introduced new variable vector, we design the nonlinear control algorithm with command-filtered backstepping technique. The proposed control law does not need the precise dynamic mathematical model of controlled plant, just depends on the real-time measurement output of the controlled plant. A two-link robot manipulator example has been presented to illustrate the effectiveness of the proposed design. In future, research topic is to modify the algorithm for high-order system while this paper is for second-order system.

Acknowledgment. This work was partially supported by the National Natural Science Foundation of China (61503156, 61473250 and 61403161), the Fundamental Research Funds for the Central Universities (JUSRP11562, NJ20150011), and the Natural Science Foundation of Jiangsu Higher Education Institution (14KJB120013).

REFERENCES

- [1] Z. Lin and A. Saberi, Semi-global exponential stabilization of linear systems subject to ‘input saturation’ via linear feedbacks, *Syst. Control Lett.*, vol.21, no.3, pp.225-239, 1993.
- [2] T. Hu and Z. Lin, *Control Systems with Actuator Saturation: Analysis and Design*, Birkhauser, Boston, MA, USA, 2001.
- [3] B. Zhou, G. Duan and Z. Lin, On semiglobal stabilization of discrete-time periodic systems with bounded controls, *IEEE Trans. Circuits Syst. II, Exp. Briefs*, vol.58, no.7, pp.452-456, 2011.
- [4] X. Liu, L. Wang, W. Yu and S. Zhong, Constrained control of positive discrete-time systems with delays, *IEEE Trans. Circuits Syst. II, Exp. Briefs*, vol.55, no.2, pp.193-197, 2008.
- [5] B. Zhou, G. Duan and Z. Lin, A parametric periodic Lyapunov equation with application in semi-global stabilization of discrete-time periodic systems subject to actuator saturation, *Automatica*, vol.47, no.2, pp.316-325, 2011.
- [6] G. Valmórbida, S. Tarbouriech and G. Garcia, State feedback design for input-saturating quadratic systems, *Automatica*, vol.46, no.7, pp.1196-1202, 2010.
- [7] H. Huang, D. Li, Z. Lin and Y. Xi, An improved robust model predictive control design in the presence of actuator saturation, *Automatica*, vol.47, no.7, pp.861-864, 2011.

- [8] D. Xu, B. Jiang and P. Shi, A novel model free adaptive control design for multivariable industrial processes, *IEEE Trans. Industrial Electronics*, vol.61, no.11, pp.6391-6398, 2014.
- [9] D. Xu, B. Jiang and P. Shi, Adaptive observer based data-driven control for nonlinear discrete-time processes, *IEEE Trans. Automation Science and Engineering*, vol.11, no.4, pp.1037-1045, 2014.
- [10] J. Farrell, M. Polycarpou and M. Sharma, Longitudinal flight path control using on-line function approximation, *AIAA J. Guid., Control Dyn.*, vol.26, no.6, pp.885-897, 2003.
- [11] J. Yao, Z. Jiao and D. Ma, Extended-state-observer-based output feedback nonlinear robust control of hydraulic systems with backstepping, *IEEE Trans. Industrial Electronics*, vol.61, no.11, pp.6285-6293, 2014.
- [12] D. Swaroop, J. Hedrick, P. Yip and J. C. Gerdes, Dynamic surface control for a class of nonlinear systems, *IEEE Trans. Automatic Control*, vol.45, no.10, pp.1893-1899, 2000.
- [13] J. Farrell, M. Polycarpou, M. Sharma and W. Dong, Command filtered backstepping, *IEEE Trans. Automatic Control*, vol.54, no.6, pp.1391-1395, 2009.
- [14] Q. Shen, P. Shi, T. Zhang and C. C. Lim, Novel neural control for a class of uncertain pure-feedback systems, *IEEE Trans. Neural Networks and Learning Systems*, vol.25, no.4, pp.718-727, 2014.
- [15] Z. Hou and Z. Wang, From model-based control to data-driven control: Survey, classification and perspective, *Inform. Sci.*, vol.235, no.20, pp.3-35, 2012.
- [16] X. Su, L. Wu, P. Shi and Y. Song, H_∞ model reduction of Takagi-Sugeno fuzzy stochastic systems, *IEEE Trans. Syst., Man, Cybern. B, Cybern.*, vol.42, no.6, pp.1574-1585, 2012.
- [17] S. Tong, P. Shi and H. Al-Madfai, Robust fuzzy decentralized control for nonlinear large scale systems with parametric uncertainties, *J. Intell. Fuzzy Syst.*, vol.19, no.2, pp.85-101, 2008.
- [18] J. Han, From PID to active disturbance rejection control, *IEEE Trans. Industrial Electronics*, vol.56, no.3, pp.900-906, 2009.
- [19] D. Xu, B. Jiang and P. Shi, Nonlinear actuator fault estimation observer: An inverse system approach via T-S fuzzy model, *Int. J. Appl. Math. Comput. Sci.*, vol.22, no.1, pp.183-196, 2012.